A DISSERTATION ON

"First Principal Study of Structural, Electronic, and Reactive Properties of Ni-O Nanoclusters"

PROJECT REPORT SUBMITTED TO THE DEPARTMENT OF PHYSICS

INTEGRAL UNIVERSITY, LUCKNOW

IN PARTIAL FULLFILLMENT FOR THE DEGREE OFMASTER OF SCIENCE

IN PHYSICS

SUBMITTED BY

MUHAMMAD HARIS

M.Sc. PHYSICS (IV SEMESTER)

ROLL NO-2101080006

UNDER THE SUPERVISION OF

PROF. POONAM TANDON

DEAN STUDENT WELFARE

DEPARTMENT OF PHYSICS

UNIVERSITY OF LUCKNOW

LUCKNOW-226026

CERTIFICATE OF ORIGINALITY

I hereby confirm that the dissertation titled " **First Principal Study of Structural, Electronic, and Reactive Properties of Ni-O Nanoclusters** " submitted by me to the Department of Physics at Integral University, Lucknow, as a partial fulfillment of the requirements for the degree of Master of Science in Physics, is the result of my independent and original research conducted at the Macromolecular Lab, Department of Physics, University of Lucknow. I affirm that this project work has not been submitted elsewhere for any other academic degree or diploma.

Name of Author(s): MUHAMMAD HARIS

 Designation: STUDENT

Affiliated Institution: INTEGRAL UNIVERSITY, LUCKNOW

Title of the Dissertation: First Principal Study of Structural, Electronic, and Reactive Properties of Ni-O Nanoclusters

Email: harismohd@iul.ac.in

DATE: **MUHAMMAD HARIS**

CERTIFICATE FROM SUPERVISOR

This is to certify that **MUHAMMAD HARIS**, a student of. **M.Sc. Physics (II Year/ IV Semester)** Integral University has completed his Dissertation work entitled "**First Principal Study of Structural, Electronic, and Reactive Properties of Ni-O Nanoclusters**" successfully. He has completed the work from University of Lucknow under Prof. Poonam Tandon, Dean student welfare at the University of Lucknow, for the partial fulfilment of the requirement for award of the degree of Master of Science. Further, this has not been submitted anywhere else for the award of any other degree or diploma.

I wish him good luck and bright future.

Dr. Seema Srivastava   **Date:**

Dean student welfare at the University of Lucknow

DEPARTMENT OF PHYSICS

LUCKNOW-226007 (U.P) INDIA

CERTIFICATE FROM INTERNAL ADVISOR

This is to certify that **MUHAMMAD HARIS**, a student of **M.Sc. Physics (II Year/ IV Semester).** Integral University has completed his Dissertation work entitled **"First Principal Study of Structural, Electronic, and Reactive Properties of Ni-O Nanoclusters"** successfully. He has completed the work from University of Lucknow under my supervision for the partial fulfilment of the requirement for award of the degree of Master of Science. Further, this has not been submitted anywhere else for the award of any other degree or diploma.

I wish him good luck and bright future.

Prof. Poonam Tandon

Dean student welfare at the University of Lucknow

ACKNOWLEDGEMENT

I would like to express my sincere gratitude and appreciation to all those who have contributed to the successful completion of my study on "**First Principal Study of Structural, Electronic, and Reactive Properties of Ni-O Nanoclusters.**" Without their support, guidance, and assistance, this research would not have been possible.

First and foremost, I extend my deepest appreciation to **Prof. Poonam Tandon, Dean student welfare at the University of Lucknow**, for providing me with the opportunity to be a part of this esteemed institution and allowing me to join her prestigious lab. Her guidance and mentorship have been invaluable in shaping my understanding and helping me achieve the project's objectives.

I am also immensely grateful to **Dr. Seema Srivastava, Head of the Department of Physics at Integral University Lucknow**, for her unwavering support, encouragement, and guidance throughout the duration of this project. Her constant motivation and belief in my abilities have been instrumental in making this endeavour exciting and fulfilling.

I am indebted to **Mr. Ashok Singh Bahota**, **a Research Scholar in the Department of Physics at the University of Lucknow**, for his exceptional mentorship and continuous support at every step of this project. His valuable suggestions and guidance have been crucial in ensuring the timely completion of the work. I am truly grateful for his kind words and invaluable assistance.

My sincere thanks go to all the members of the **Department of Physics at Integral University, Lucknow,** who generously dedicated their time and offered guidance, contributing to the success of this project. Additionally, I would like to express my gratitude to all the members of the **Macromolecular Lab in the Department of Physics at the University of Lucknow** for their unwavering support and assistance throughout the course of my project.

Lastly, I would like to extend a special token of appreciation to my family and friends whose unwavering support, encouragement, and blessings have been a constant source of motivation throughout my academic journey.

I am sincerely thankful to everyone mentioned above for their invaluable contributions, guidance, and support. Without their assistance, this project would not have been possible.

MUHAMMAD HARIS

TABLE OF CONTENTS

LIST OF SYMBOLS AND ABBREVIATIONS

BO = Born-Oppenheimer Approximation

HF = Hartree-Fock Theory

HOMO-Highest Occupied Molecular Orbital

LUMO- Lowest Unoccupied Molecular Orbital

DFT = Density Functional Theory

E = Energy

ρ = (rho) Ground State Energy of the system

ρ (r) = Electron Density Matrix

Σ = Sigma

Ψ = wave function

$E_{CORRELATION}$ = Correlation Energy

$E_{EXACT\ ENERGY}$ = Exact Energy

E_{HF} = Energy of the System in HF Model

ε_i = Epsilon sign (Kohn-Sham Orbital Energy)

V_{XC} = Function Derivative of the Exchange-Correlation Energy

χ = Electronegativity

μ = Chemical Potential

η = Global Hardness

S = Global Softness

ω = Electrophilicity Index

E_H = HOMO Energy, E_L = LUMO Energy

CHAPTER 1. INTRODUCTION

1.1 NANOMATERIALS

Nanomaterials refer to materials that have structural components or features at the nanoscale, typically ranging from 1 to 100 nanometers. They can be engineered or naturally occurring and can exhibit unique properties and behaviours due to their small size and large surface area-to-volume ratio.
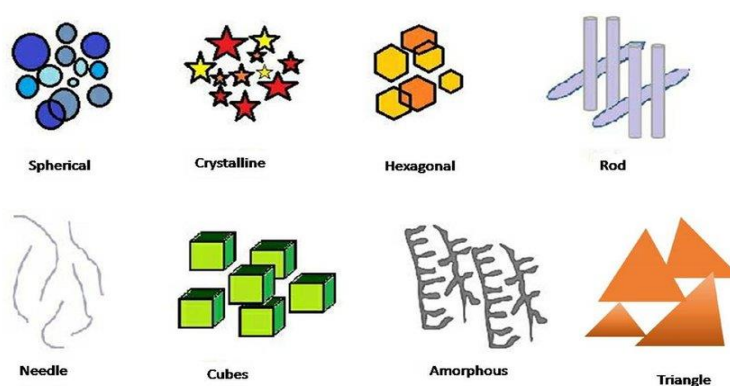

Fig 1.1. An example showing different types and shapes of nanomaterials

1.2 NANOCLUSTERS

A nanocluster refers to a small assembly of atoms or molecules, typically ranging in size from a few to a few hundred atoms. These clusters exhibit unique physical and chemical properties that can differ from those of individual atoms or bulk materials. Nanoclusters can be composed of various elements and can be found in different forms such as metallic, semiconductor, or organic clusters [1].

Nano-clusters have peculiar properties because they are finite small objects. Nano-clusters are well suited for various applications, whose number is rapidly increasing because of very favourable surface/volume ratio of Nano clusters.

For optimization of Nano-cluster synthesis method gives rapid, quantitative feedback concerning final cluster size, shape, optical properties and their relationship to the myriad synthetic variables is necessary [2].
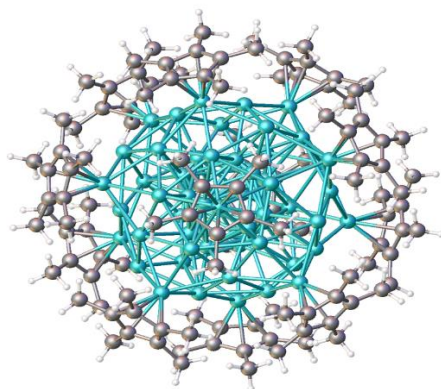
Fig 1.2. An example of a nanocluster ($Cp*_{10}Al_{50}$)

It is well known that advances in organic synthesis have been facilitated greatly by the advent of modern analysis methods, such as Fourier Transform Infrared Spectroscopy (FTIR), gas chromatography/ mass spectrometry (GC/MS), liquid chromatography (LC) using photodiode array absorbance measurements (LC/PDA), nuclear magnetic resonance (NMR). Without such feedback, the synthetic chemist is ignorant with respect to whether changes in synthetic protocol arte improving the final product [3].

PROPERTIES OF NANOCLUSTER

The key characteristics of nanoclusters is their size-dependent behaviour, where their properties vary based on their size. This size-dependent behaviour arises due to quantum confinement effects, which lead to discrete energy levels and altered electronic properties as the size of the nanocluster decreases [4]. Additionally, nanoclusters have a high surface-to-volume ratio, resulting in a large surface area relative to their volume [3]. This high surface area enables increased interactions with the surrounding environment, making nanoclusters highly reactive and providing more sites for chemical reactions or adsorption of molecules [5]. Their small size also leads to enhanced reactivity compared to bulk materials. Nanoclusters exhibit tunable properties, allowing for precise control over their characteristics by modifying factors such as size, composition, and surface ligands.

Furthermore, nanoclusters can adopt a variety of structures depending on their size, composition, and synthesis conditions, affecting their physical and chemical properties.

Quantum effects become more prominent at the nanoscale, influencing the behaviour of nanoclusters [6]. These effects include the quantization of electronic energy levels, quantum tunneling, and wave-particle duality.

The interplay of these properties makes nanoclusters highly versatile and attractive for applications such as catalysis, electronics, energy conversion, sensing, and biomedical imaging [2]. Ongoing research aims to further understand and harness the unique properties of nanoclusters for the development of advanced materials and technologies

1.3 METAL NANOCLUSTER

Metal nanoclusters are nanoscale assemblies of metal atoms. They consist of a small number of metal atoms, typically ranging from a few to a few hundred atoms, and exhibit unique properties that are distinct from both individual metal atoms and bulk metal materials [7]. Metal nanoclusters can be composed of various metals such as gold, silver, platinum, copper, and many others.
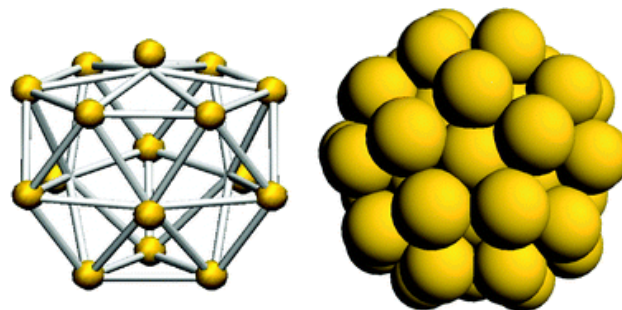
Fig 1.3. Atomic structure of Gold nanoclusters.

1.4 NANOCLUSTER SYNTHETIC METHOD
Sol-Gel Method

The sol-gel method involves dissolving metal alkoxides, known as metal precursors, in water to form a solution. This solution undergoes a gelation process through hydrolysis or alcoholysis [3]. The resulting gel is initially wet or damp and requires appropriate drying methods tailored to the desired properties and applications. For instance, if the

solution contains alcohol, the drying can be achieved by burning off the alcohol. Once dried, the gels are powdered and subsequently calcined [8].

The basis of the sol-gel method is the production of HOMOgenous solution from a precursor and its conversion into a gel.
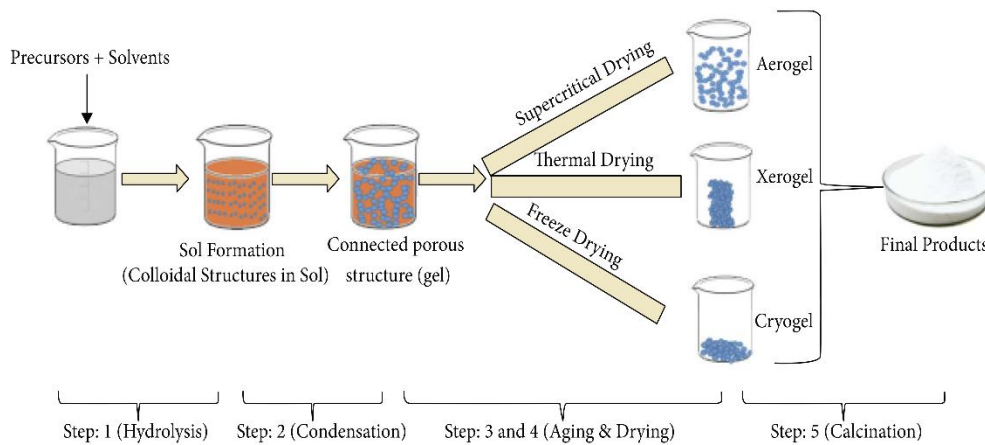

Fig 1.4. Schematic of different stages of sol-gel process: from precursor to aerogel.

1.5 Synthesis of Ni-O Nanocluster

Ni-O nanoclusters are synthesized via the sol-gel method using nickel alkoxides dissolved in alcohol solvents. The precursor solution is hydrolyzed by adding water or a hydrolyzing agent, forming nickel hydroxide species. Gelation occurs through aging the solution, allowing for particle growth. The resulting wet gel is dried using evaporation or freeze-drying to remove solvents and water. Subsequent calcination converts the nickel hydroxide into Ni-O nanoclusters [9]. The synthesized nanoclusters can be characterized and further processed for applications such as catalysts, sensors, or energy storage. Optimization of synthesis parameters may be necessary to achieve desired properties. Overall, this method offers a route for fabricating Ni-O nanoclusters with controlled properties. The sol-gel method offers control over the size, composition, and properties of the nanoclusters, making it a versatile approach for the synthesis of Ni-O nanoclusters with tailored characteristics [10].

1.6 Applications of Nanoclusters

Nanoclusters, which are tiny clusters of atoms or molecules with nanoscale dimensions, find applications across various fields due to their unique properties. Some common applications of nanoclusters include:

(a) Catalysis: Nanoclusters serve as highly efficient catalysts due to their high surface area-to-volume ratio, enabling enhanced reactivity and selectivity in chemical reactions. They are utilized in catalytic converters, fuel cells, and chemical synthesis processes**.**

(b) Surface Coatings and Thin Films: Nanoclusters can be incorporated into coatings and thin films to enhance surface properties such as hardness, corrosion resistance, and self-cleaning capabilities.
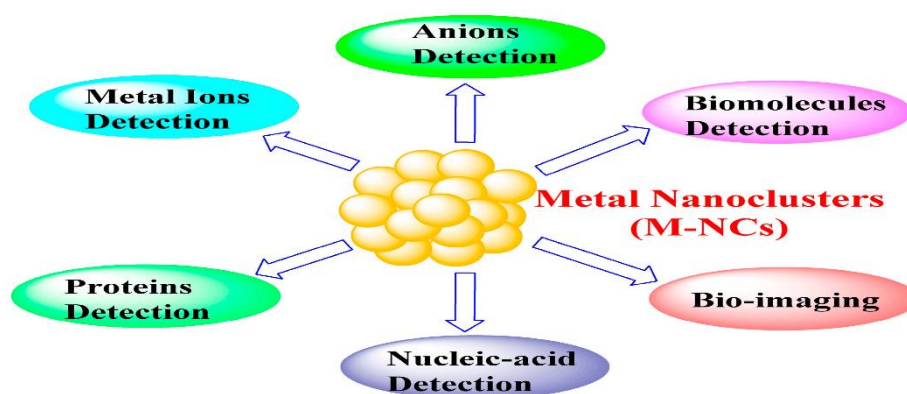
Fig 1.5. Various application of metal nanoclusters.

(c) Sensing and Detection: Nanoclusters enable highly sensitive and selective sensing and detection of various analytes, including gases, chemicals, and biological molecules. They are utilized in gas sensors, biosensors, and environmental monitoring devices**.**

(d) Biomedical Imaging: Nanoclusters can be functionalized and utilized as contrast agents in biomedical imaging techniques such as magnetic resonance imaging (MRI), computed tomography (CT), and fluorescence imaging.

(e) Energy Storage: Nanoclusters are employed in energy storage applications such as batteries, supercapacitors, and hydrogen storage.

CHAPTER 2. REVIEW OF LITERATURE

2.1 Study by Palanisamy and Raichur

Recently, researchers Palanisamy and Raichur utilized two different microemulsion approaches to synthesize Ni-O nanoparticles. They initially formed Ni(OH)2 particles, which were then subjected to calcination at 600°C, resulting in the production of nickel oxide (Ni-O) particles measuring 47 nm. Another group led by Gao employed a microwave-assisted method to synthesize Ni-O nanorods composed of numerous Ni-O nanoparticles. They achieved this by thermally decomposing a rod-like nickel oxide precursor . Rodríguez-Llamazares et al. devised a method based on ligand displacement of bis(1,5-cyclooctadiene)-nickel(0), a zero valent organometallic precursor, and the simultaneous formation of a thiourea inclusion compound to synthesize nickel/nickel oxides nanoparticles . In this study, the objective is to synthesize relatively small Ni-O nanoclusters quickly and easily using a simple and non-toxic precursor, employing a low-temperature, low-cost method that does not require any special instruments.

2.2 Copper Nanoclusters

Considerable research efforts have been dedicated to the characterization and properties of copper nanoclusters in recent years. Several highly effective synthetic methods have been developed to prepare copper nanoclusters, and their successful synthesis has been confirmed through electron microscopy and mass spectrometry. Electrochemical and wet chemical reduction techniques have been employed to synthesize stable copper nanoclusters smaller than Cu13 and Cu8, respectively. These synthesized copper nanoclusters possess distinctive fluorescent and catalytic properties. However, despite the advancements made in this field, further research is still necessary to explore the potential of copper nanoclusters fully. In previous studies, hydrophobic Cu nanoclusters with varying core sizes have been predominantly synthesized. Therefore, a critical focus lies in obtaining monodispersed and stable water-soluble copper nanoclusters, as this is crucial for their application in fluorescence analysis and cellular biology.

CHAPTER 3. METHODOLOGY

3.1 Theoretical Methods

Two primary theoretical methods used in the study of Ni-O nanoclusters are Molecular Mechanics and ab-initio methods. These methods are employed to understand the structural and electronic properties of the nanoclusters.

3.1.1 Molecular Mechanics (non-computational)

Molecular Mechanics is a computational method that utilizes classical physics principles to predict the structure and properties of molecules. By employing potential functions derived from classical physics, it calculates the potential energy surface for a specific arrangement of atoms [6]. These potential functions collectively form a force field, which serves as a set of equations to describe the interactions between atoms in the molecule. Through Molecular Mechanics, researchers can gain insights into the molecular structure and characteristics, enabling the investigation of various properties and behaviours of molecules [11].

3.1.2 Ab-Initio Method

The term "ab initio," originating from Latin, signifies "from the beginning." It refers to a theoretical approach that relies solely on quantum mechanics principles, without incorporating experimental data. Ab initio methods aim to solve the time-independent Schrödinger equations and generate a wave function that accurately represents the system being studied [12]. These methods are based on fundamental principles rather than relying on empirical data. Quantum chemistry employs various ab initio techniques to analyse and predict the properties of molecules and materials, providing a deep understanding of their electronic structure and behaviour. By starting from first principles, ab initio methods offer a comprehensive and theoretical framework for investigating complex systems.

3.2 Born-Oppenheimer Approximation

The Born-Oppenheimer approximation is a fundamental concept in the methodology of computational chemistry. It is based on the assumption that the motion of atomic nuclei and electrons in a molecule can be treated separately due to their significant difference

in mass. According to this approximation, the electronic motion occurs on a much faster timescale compared to the nuclear motion [9].

Born-Oppenheimer approximation (BO) is the most known mathematical approximation which assumes that the motion of atomic nuclei and the electrons can be considered separately based on the fact that the nucleus is heavier than an electron. It is assumed that the nucleus moves more slowly than the electrons [13]. Therefore, at any given instant the electron will feel a Hamiltonian that depends on the position of the nuclei.

$$\widehat{H} = -\frac{1}{2}\sum_j \nabla_i^2 + \frac{1}{2}\sum ij \frac{1}{ri_j} - \sum ij \frac{Z_I}{r_i - R_I} \qquad \dots\dots(3.1).$$

3.3 Hartfree-Fock (HF) Theory

The Hartree-Fock (HF) method is a widely used approximation in computational physics and chemistry to calculate the wave function and energy of a stationary quantum many-body system. The HF method not only determines the wave function but also provides the energy of the quantum system. It was developed to solve the electronic Schrödinger equation, which arises from the time-independent Schrödinger equation when applying the Born-Oppenheimer approximation [14].

In the HF method, the objective is to find the set of spin orbitals that minimizes the energy and represents the "best single determinant" for the system. However, to simplify the calculations, certain approximations are made within the HF method.

Overall, the HF method is a useful tool for investigating the electronic structure and properties of many-body systems, allowing researchers to obtain valuable insights into the behaviour of molecules and materials [10].

HF method determines the set of spin orbitals which minimize the energy and give us the "best single determinant". To deal with the task some approximations are made by the HF method.

(a) Born-Oppenheimer approximation.

(b) LCAO-MO approximation.

Hamiltonian for many-body systems can be written as:

$$\widehat{H}\Psi = E\Psi \quad \dots\dots\dots\dots(3.2)$$

$$\hat{H} = T + V \quad \ldots\ldots\ldots\ldots..(3.3)$$

$$\hat{H} = -\frac{1}{2}\sum_{i}^{nuclei}\frac{1}{M_I}\nabla_i^2 - \frac{1}{2}\sum_{j}^{electrons}\nabla_i^2 + \frac{1}{2}\sum_{ij}^{nuclei}\frac{Z_I Z_j}{R_{Ij}} + \frac{1}{2}\sum_{Ij}^{electrons}\frac{1}{r_{ij}} - \sum ij \frac{Z_I}{r_i - R_I}$$

$\ldots\ldots..(3.4)$

HF method completely neglect the electron correlation therefore this can't be used accurately used in the process where the total number of paired electrons changes.

3.4 Density Functional Theory

Density Functional Theory (DFT) is a widely utilized computational technique for determining the structure and interactions of atoms, molecules, crystals, and other systems "ab initio" (from first principles) [11]. Unlike wavefunction-based approaches, DFT is based on the density of the electrons rather than their individual wavefunctions. Its primary objective is to approximate the solution of the Schrödinger equation in order to determine the ground state of a many-body system.

In summary, DFT is a powerful computational tool based on the density of electrons. It provides a practical means of approximating the ground state of many-body systems and calculating their properties by employing functionals of the electron density [15]. The development of the Hohenberg-Kohn theorems has laid the foundation for the theoretical understanding and application of DFT in a wide range of scientific investigations.

3.5 The Hohenberg-Kohn Theorem

This can be applied to any system consisting of electrons moving in the influence of external potential.

3.5.1 First Hohenberg-Kohn Theorem

According to the first Hohenberg-Kohn theorem, all ground state properties of a system can be determined solely by its density i.e

$$E = E[\rho] \quad \ldots\ldots\ldots(3.5)$$

Where ρ is the ground state density of the system.

3.5.2 Second Hohenberb-Kohn Theorem

The second Hohenberg-Kohn theorem establishes the existence of a variational principle for the energy density functional, denoted as E[ρ]. This principle demonstrates that the density, ρ, used in the functional is not necessarily the ground state density of the system [16].

$$E = E[\rho'] > E[\rho] \quad \text{...............(3.6)}$$

In HF models, the energy of the system, E_{HF} is written as:

$$E_{HF} = E_{core} + E_{nuclear} + E_{columb} + E_{exchange}$$

The exchange correlation energy are determined as an integral of some function of the total electron density.

$$E_{XC} = \int \rho(r) Exc[\rho(r)] dr$$

The electron density matrix ρ(r) is determined from Kohn-Sham orbitals Ψ.

$$\rho(r) = \sum_{i=1}^{N} |\Psi_1|^2$$

The Kohn-Sham wavefunctions are determined from Kohn-Sham Equations

$$\left(\frac{1}{2} \nabla_i^2 - \sum_i^{nuclei} \frac{Z_a}{R_{A.1}} + \int \frac{\rho(r)_2}{r_{12}} dr_2 + V_{xc}(r_1) \right) \Psi_i(r)_i = \epsilon_i \Psi_i(r_i)$$

The term ϵ_i are the Kohn-Sham orbitals energies. The correlation-exchange potential V_{XC} is the functional derivative of the exchange correlation energy.

$$V_{XC}[\rho] = \frac{E_{XC}[\rho]}{\delta\rho}$$

The wavefunction Ψ of a system with N electrons involves 3N variables, whereas the system's density is described by only 3 variables (x, y, z). Transitioning from evaluating E(Ψ) to E(ρ) in computational chemistry significantly decreases the computational burden required to analyze the electronic properties, electronegativity, chemical

potential, hardness, softness, Fukui functions, and other characteristics of atoms, molecules, and solids [12].

3.6 Basis Set

In theoretical and computational chemistry, a basis set comprises a collection of functions known as basis functions. These basis functions are combined through linear combinations with coefficients to form molecular orbitals. The purpose of a basis set is to represent the electronic wave function in methods such as the HF method or density-functional theory [13]. By employing a basis set, the partial differential equations of the model are transformed into algebraic equations, enabling efficient computational implementation on a computer [17].

A basis set is a set of wave functions that describes the shape of atomic orbitals (AOs). The molecular orbitals (MOs) are computed using the selected theoretical model by linearly combining the AOs (LCAO). Not all theoretical model requires the user to choose a basis set to work with [14].

3.7 Pople Basis Set

Pople basis sets, named after John Pople, are widely used sets of basis functions in computational chemistry. These basis sets are specifically designed to approximate the electronic wave functions of atoms and molecules accurately. Pople basis sets consist of a combination of Gaussian-type orbitals (GTOs) that are tailored to represent different atomic and molecular orbitals [18].

Pople basis sets are developed with varying levels of sophistication, including single-zeta (SZ), double-zeta (DZ), triple-zeta (TZ), and quadruple-zeta (QZ) sets [9].

Here is a list of commonly used split-valence basis sets of this type.

(a). 3-21G

(b) 3-21G*-polarization function on heavy atoms

(c) 3-21G**- polarization functions on heavy atoms and hydrogen

(d) 3-21+G. - Diffuse functions on heavy atoms

(e) 3-21++G- Diffuse functions on heavy atoms and hydrogen

(f) 4-21G

(g) 4-31G

(h) 6-21G

(i) 6-311++G*

All the calculations have been performed with Gaussian16.

After that, following formulas were used to calculate global and local reactivity descriptor

$$\chi = \frac{1}{2}(\epsilon_{LUMO} + \epsilon_{HOMO})$$

$$\mu = -\frac{1}{2}(\epsilon_{LUMO} + \epsilon_{HOMO})$$

$$\eta = \frac{1}{2}(\epsilon_{LUMO} - \epsilon_{HOMO})$$

$$S = \frac{1}{2\eta}$$

$$\omega = \frac{\mu^2}{2\eta}$$

Where Electrophilicity index (ω) measures the stabilization in energy. The energies of frontier molecular orbitals (E_{HOMO}, E_{LUMO}), energy gap (E_{LUMO}-E_{HOMO}), electronegativity (χ). chemical potential (μ), global hardness (η), global softness (S), and global electrophilicity index (x) for reactants [15].

3.8 LanL2DZ Basis Set.

The LanL2DZ basis set is utilized for evaluating the electronic structure of d-group elements. It comprises an effective core potential to account for core electrons and an all-electron basis set to describe valence electrons [16]. For elements in groups 14-17, the LanL2DZ basis set incorporates optimized diffuse and polarization functions. These optimized exponents are generally similar to those obtained using different effective core potentials, valence basis sets, or computational models. The best generalized sets of exponents are determined by averaging results from different models [19]. When

employed with the B3LYP model, the extended LanL2DZ basis sets yield good results for atomic electron affinities, with an average deviation of 0-11 eV from experimental values.

However, the performance is consistently lower when used with the MP2 model. In calculations of vibrational frequencies and bond energies for selected main group compounds, the extended LanL2DZ basis sets show similar performance to the all-electron 6-31+G(d) basis set and offer intermediate computational speed between the 6-31+G(d) basis set and the unmodified LanL2DZ basis set.

In this present work we have taken the atoms of Nickel (Ni) and Oxygen(O) and through Gaussian the structures from Ni2O2 to Ni9O9 were optimized at **B3LYP** under **LanL2DZ** Basis Set [20].

CHAPTER 4. RESULTS AND DISCUSSION

4.1 STRUCTURE ANALYSIS

Through ABCluster3.0 we obtained ten structures of each $[Ni_nO_n$ (n=2-9)] nanostructures. And further with Gaussian we optimized the best stable structure using DFT method under B3LYP/LanL2DZ level of theory.

Following figures represent the structures of Ni2O2 to Ni9O9.

Ni Atom   O Atom

Ni2O2
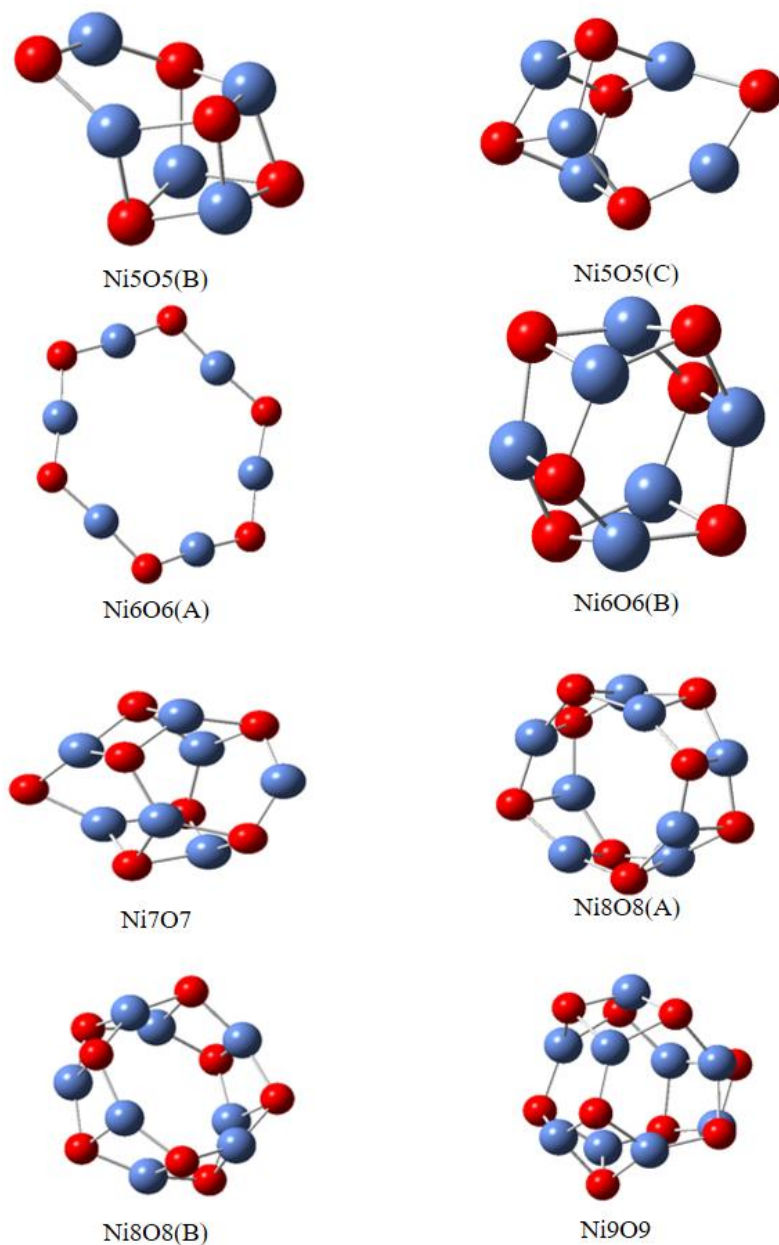
Ni3O3(A)

Ni3O3(B)

Ni4O4(A)

Ni4O4(B)

Ni4O4(C)

Ni5O5(A)
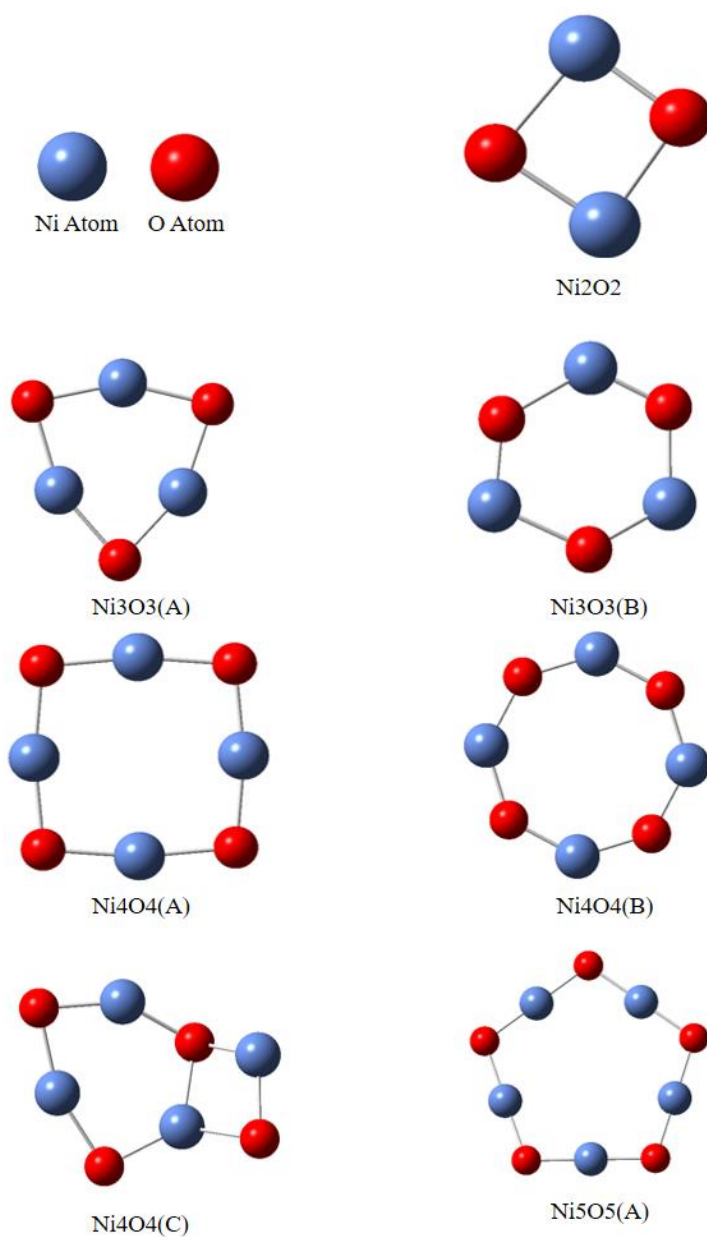
Fig 4.1. Optimized Structure of Ni_nO_n (n=2-9) Nanoclusters with B3LYP/LanL2DZ level of Theory. Here, the blue and red atom represents Nickel and Oxygen atom respectively.

From the figure 4.1, it is clear that- Ni_2O_2 has a cubic crystal structure. In this case, the nickel and oxygen atoms are arranged in 2D. The point group symmetry of Ni_2O_2 here is C1. Both compounds of Ni_3O_3 i.e. $Ni_3O_3(A)$ and $Ni_3O_3(B)$ are planar or 2D showing triangle and hexagonal like structure and has point group symmetry of C1.

Ni4O4 structures (A), (B) and (C) have square, circle and random shape and these all the planar form having point group symmetry C1. Ni5O5 structures (A), (B) and (C) has point group symmetry C1 and compound Ni5O5(A) has planar arrangement while compounds Ni5O5(B) and Ni5O5(C) are in 3D shape. Here compound Ni6O6 are optimized in two compounds (A) and (B) of which Ni6O6(A) is planar while Ni6O6(B) is in 3D and possess point group symmetry of C1. The optimization state of Ni7O7 possess 3D structure with point group symmetry of C2. The structures of Ni8O8(A), Ni8O8(B) as well as Ni9O9 all possess 3D structure with point group symmetry of C2V, C2V and C1 respectively.

4.2 BOND LENGTH

Bond length refers to the distance between the nuclei of two bonded atoms in a molecule. It represents the equilibrium distance at which the attractive and repulsive forces between the atoms are balanced. Bond length is typically measured in units of length, such as angstrom (Å) or picometers (pm) [11].

By computational analysis the bond lengths from **Ni2O2 to Ni9O9** is provided below.

1. **Ni2O2:** The average bond length ranges from 1.799 to 1.801 Å.

2. **Ni3O3(A):** The average bond length ranges from 1.744 to 1.762 Å.

3. **Ni3O3(B):** The average bond length ranges from 1.743 to 1.763 Å.

4. **Ni4O4(A):** The average bond length is 1.735 Å.

5. **Ni4O4(B):** The average bond length is 1.727 Å.

6. **Ni4O4(C):** The average bond length ranges from 1.735 to 1.918 Å.

7. **Ni5O5(A):** The average bond length ranges from 1.691 to 1.729 Å.

8. **Ni5O5(B):** The average bond length ranges from 1.750 to 2.565 Å.

9. **Ni5O5(C):** The average bond length is the same as Ni5O5(b).

10**. Ni6O6(A):** The average bond length is 1.708 Å.

11**. Ni6O6(B):** The average bond length ranges from 1.809 to 1.858 Å.

12. **Ni7O7:** The average bond length ranges from 1.777 to 1.968 Å.

13**. Ni8O8(A):** The average bond length ranges from 1.800 to 2.056 Å.

14**. Ni8O8(B):** The average bond length is the same as Ni8O8(a).

15. **Ni9O9:** The average bond length ranges from 1.770 to 1.900 Å.

As the cluster size increases, there is a general decreasing trend in the average bond lengths. This indicates a contraction of the bond lengths as more Ni and O atoms are incorporated into the clusters.

Ni-O nanoclusters with smaller sizes, such as Ni2O2 and Ni3O3, have longer average bond lengths compared to larger clusters, indicating less compact bonding potentially influenced by surface effects.

Ni4O4(A) and Ni4O4(B) exhibit a slight decrease in average bond length compared to Ni3O3, indicating further bond contraction. Ni4O4(C) shows a wider range of average bond lengths, indicating structural variability within the cluster ensemble. Ni5O5(A) demonstrates a shorter average bond length range compared to Ni4O4 clusters, suggesting further bond contraction with the addition of more Ni and O atoms. Ni5O5(B) and Ni5O5(C) also display a wider range of average bond lengths, indicating structural variability similar to Ni4O4(C).

Ni6O6(A) exhibits a relatively short average bond length, possibly due to increased bonding within the cluster. Ni6O6(B) exhibits a wider range of average bond lengths, similar to previous cases, suggesting structural variability.

Ni7O7 demonstrates a wider range of average bond lengths, indicating structural diversity within the cluster ensemble. Ni8O8(a) and Ni8O8(b) show a wider range of average bond lengths, suggesting structural variability within the cluster ensemble.

Finally, Ni9O9 exhibits a relatively narrow range of average bond lengths, indicating a more consistent bond length within the cluster.

Overall, the data suggests that as the cluster size increases, the average bond lengths tend to decrease, reflecting a greater compactness and increased bonding within the nanoclusters. However, structural variability is also observed within certain cluster sizes, indicating different conformations or arrangements of Ni and O atoms within the clusters.

4.3 HOMO-LUMO Analysis

The HOMO-LUMO analysis of Ni-O nanoclusters involves studying the highest occupied molecular orbital (HOMO) and the lowest unoccupied molecular orbital (LUMO) of the clusters. These orbitals provide insights into the electronic structure and properties of the nanoclusters.

Analyzing the HOMO allows us to understand the stability and reactivity of the nanoclusters. A well-separated HOMO-LUMO gap indicates a higher stability and a lower tendency for electron transfer or reactivity. On the other hand, a smaller HOMO-LUMO gap or overlapping orbitals suggests increased reactivity and potential for electronic transitions.

Furthermore, the HOMO and LUMO energies can be used to calculate important parameters such as ionization potential (IP), electron affinity (EA), chemical potential, global hardness, electronegativity, global softness, and global electrophilicity index. These parameters provide valuable information about the clusters' chemical reactivity, energy levels, and potential applications [22].

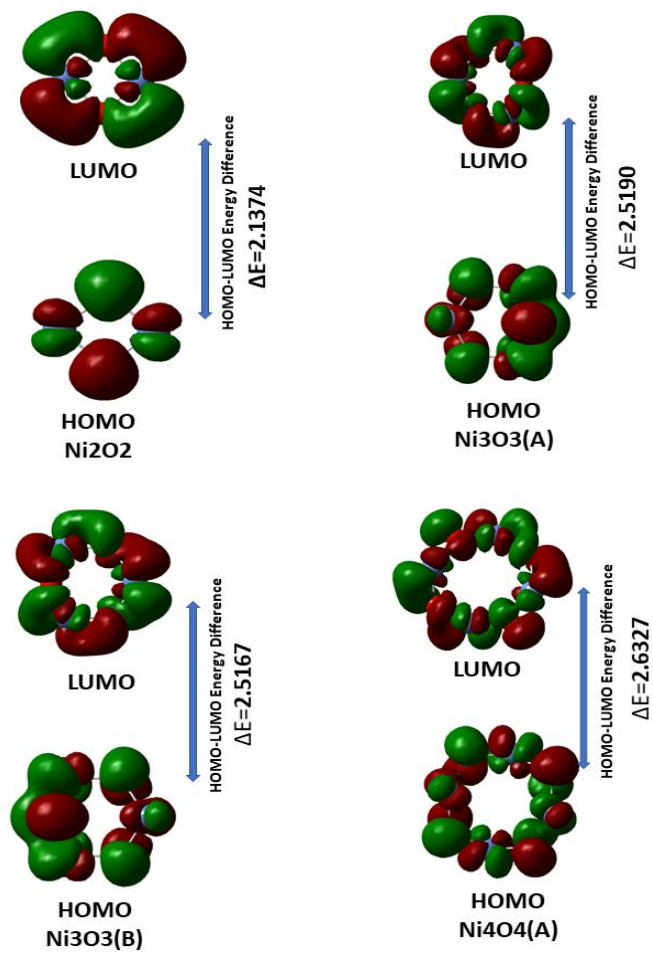Following Figure represent HUMO-LUMO Gap of Ni-O Nanocluster.

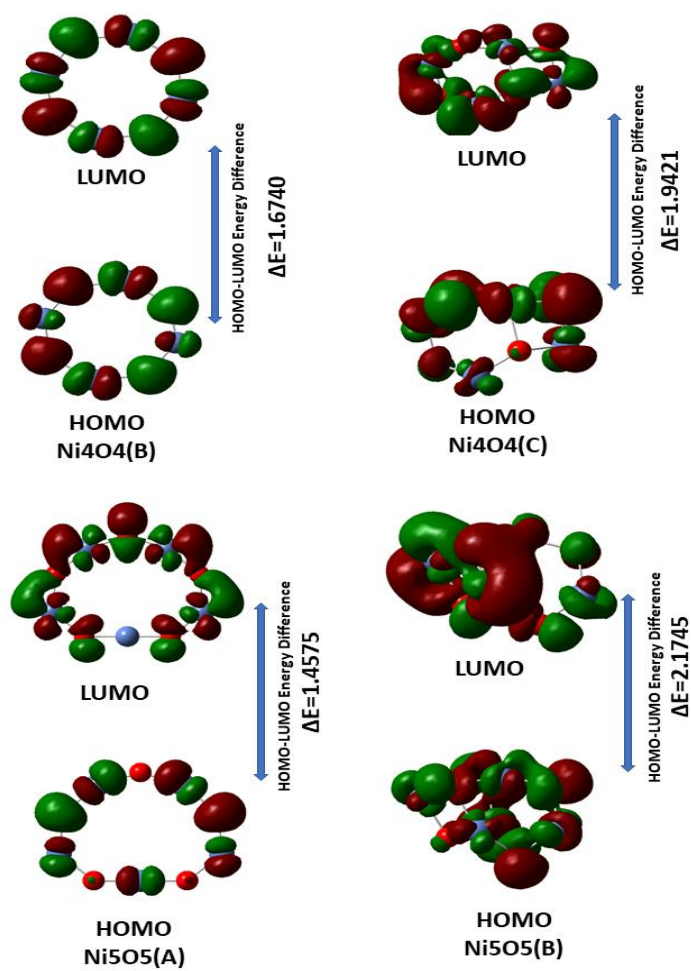Fig 4.2. HOMO-LUMO Energy Structure, and their energy difference of Ni2O2 to Ni4O4(A) nanocluster

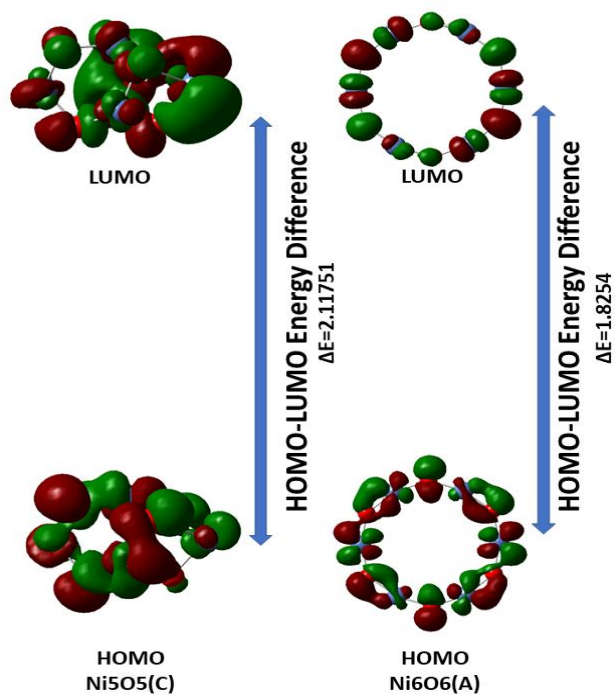Fig 4.3. HOMO-LUMO Energy Structure, and their energy difference of Ni4O4(B) to Ni5O5(B)

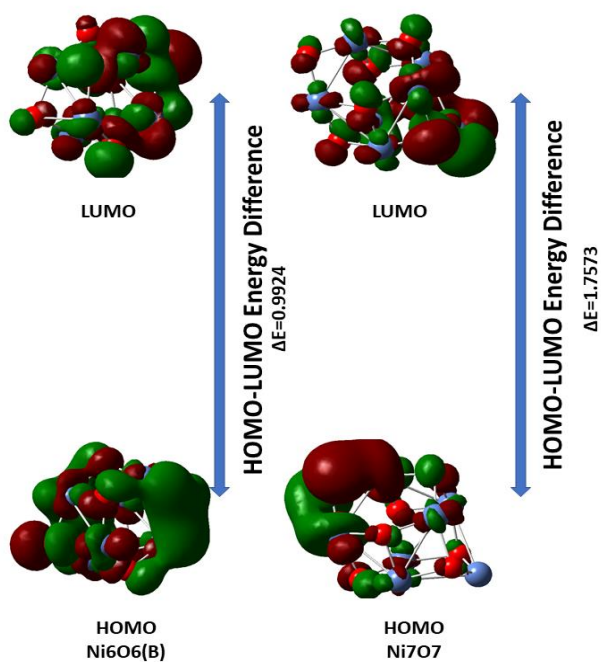Fig 4.4. HOMO-LUMO Energy Structure, and their energy difference of Ni5O5(C) to Ni6O6(A) nanocluster

Fig 4.6 HOMO-LUMO Energy Structure, and their energy difference of nanocluster Ni6O6(B) to Ni7O7
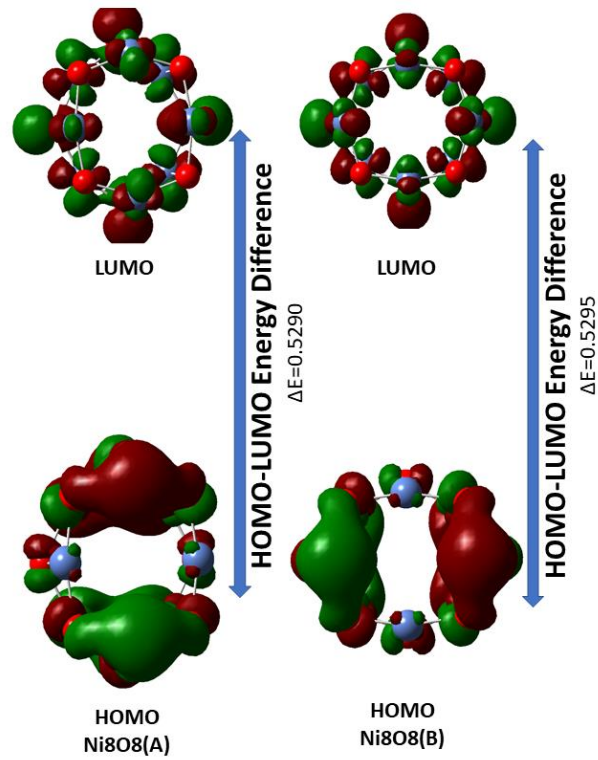
Fig 4.7 HOMO-LUMO Energy Structure, and their energy difference Ni8O8(A) to
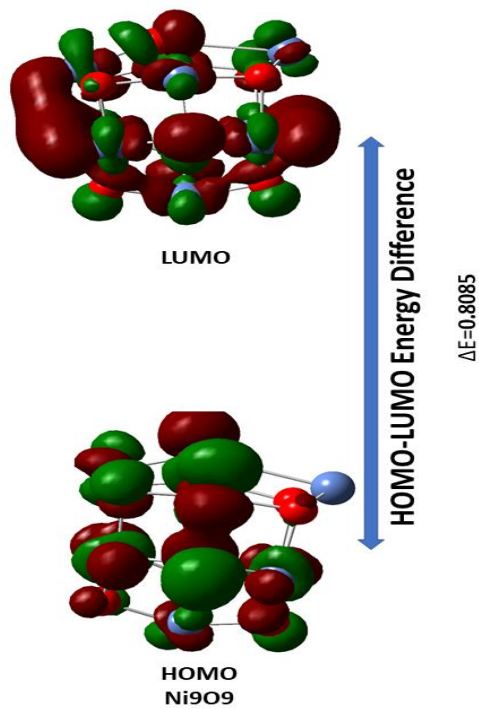Ni8O8(B) nanocluster

Fig 4.8 HOMO-LUMO Energy Structure, and their energy difference of Ni9O9
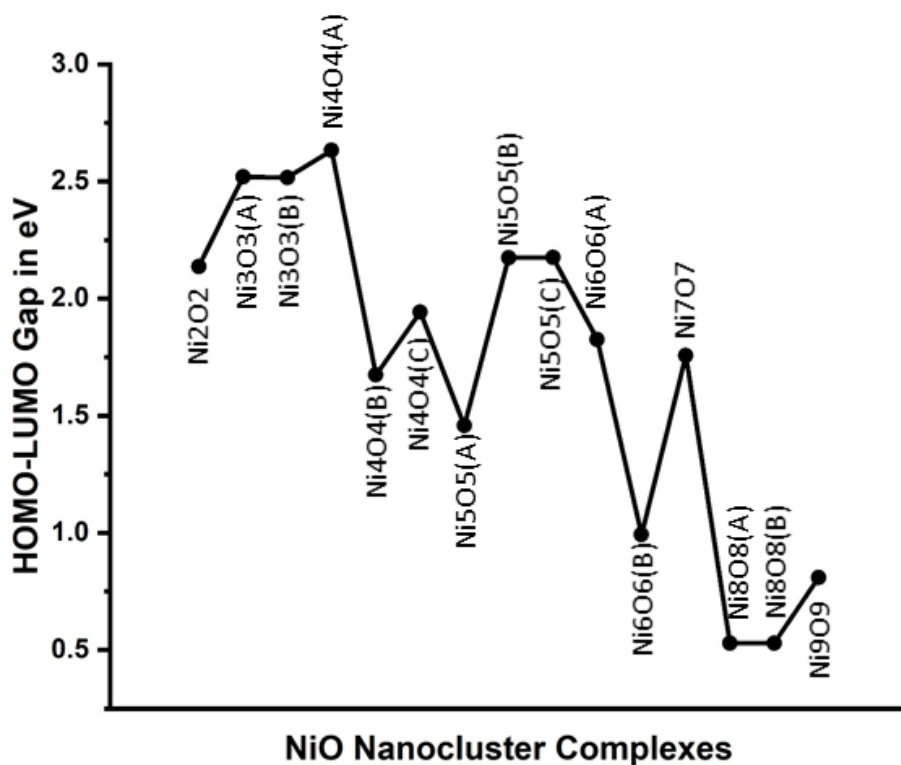nanocluster.

Fig 4.9 HOMO-LUMO energy difference of Ni-O nanocluster.

Here are some observations based on the above data:

The energy differences range from relatively small values, such as 0.5290 to 0.5295, to larger values, such as 2.6327. These differences suggest variations in the band gaps and reactivity of the nanoclusters. Nanoclusters with larger HOMO-LUMO energy differences, such as Ni4O4(A) and Ni2O2, tend to have wider band gaps, indicating higher stability and lower reactivity. These nanoclusters may have less potential for electronic or chemical transformations.

On the other hand, nanoclusters with smaller energy differences, such as Ni6O6(B) and Ni8O8(A)/(B), suggest narrower band gaps and higher reactivity. These nanoclusters may exhibit more favorable conditions for electronic transitions or chemical reactions.The trend in the HOMO-LUMO energy differences is not strictly linear or consistent.

.

4.4 FRONTIER MOLECULAR ORBITAL ANALYSIS (FMO)

Frontier molecular orbitals (FMOs) play a crucial role in understanding the electronic properties and reactivity of molecules.[23] It helps in understanding various properties such as ionization potential, electron affinity, chemical potential, global hardness, electronegativity, global softness, and global electrophilicity index, which are all influenced by the HOMO and LUMO energies [18].

Table 4.1: Table for HUMO, LUMO and calculation of HOMO-LUMO gap, ionisation potential and electron affinity.

Complex	HOMO	LUMO	Gap	Ionisation Potential	Electron Affinity
Ni2o2	-5.8281	-3.6907	2.1374	5.8281	3.6907
Ni3o3(A)	-6.4962	-3.9772	2.5190	6.4962	3.9772
Ni3o3(B)	-6.4950	-3.9783	2.5167	6.4950	3.9783
Ni4o4(A)	-6.7424	-4.1097	2.6327	6.7424	4.1097
Ni4o4(B)	-6.5144	-4.8404	1.6740	6.5144	4.8404
Ni4o4(C)	-6.1109	-4.1688	1.9421	6.1109	4.1688
Ni5o5(A)	-6.4690	-5.0115	1.4575	6.4690	5.0115
Ni5o5(B)	-6.3814	-4.2069	2.1745	6.3814	4.2069
Ni5o5(C)	-6.3820	-4.2069	2.1751	6.3820	4.2069
Ni6o6(A)	-6.9683	-5.1429	1.8254	6.9683	5.1429
Ni6o6(B)	-6.7400	-5.7476	0.9924	6.7400	5.7476
Ni7o7	-6.5563	-4.799	1.7573	6.5563	4.799
Ni8o8(A)	-6.0945	-5.5655	0.5290	6.0945	5.5655
Ni8o8(B)	-6.0948	-5.5653	0.5295	6.0948	5.5653
Ni9o9(A)	-5.4023	-4.5938	0.8085	5.4023	4.5938

Table 4.2: Table for calculation of Electrophilicity index (ω), electronegativity (χ). chemical potential (μ), global hardness (η), global softness (S).

Complex	μ	η	χ	S	ω
Ni2o2	-4.7594	1.0687	4.7594	0.467858	10.59787
Ni3o3(A)	-5.2367	1.2595	5.2367	0.396983	10.88647
Ni3o3(B)	-5.2367	1.25835	5.2367	0.397346	10.89621
Ni4o4(A)	-5.4261	1.31635	5.4261	0.379838	11.1832
Ni4o4(B)	-5.6774	0.837	5.6774	0.597372	19.255
Ni4o4(C)	-5.1399	0.97105	5.1399	0.514907	13.60283
Ni5o5(A)	-5.7403	0.72875	5.7403	0.686106	22.60753
Ni5o5(B)	-5.2942	1.08725	5.2942	0.459876	12.88941
Ni5o5(C)	-5.2945	1.08755	5.2945	0.459749	12.88732
Ni6o6(A)	-6.0556	0.9127	6.0556	0.547825	20.08891
Ni6o6(B)	-6.2438	0.4962	6.2438	1.007658	39.28359
Ni7o7	-5.6777	0.87865	5.6777	0.569055	18.34389
Ni8o8(A)	-5.8300	0.2645	5.8300	1.890359	64.25123
Ni8o8(B)	-5.8301	0.26475	5.8301	1.888574	64.19166

Ni9o9(A)	-4.9981	0.40425	4.9981	1.236858	30.89735

In this section, we review the frontier molecular orbitals of Ni-O (Nickel Oxide) and their significance in its chemical behaviour.

4.4.1 IONISATION POTENTIAL

The ionization potential refers to the energy required to remove an electron from a neutral species, resulting in the formation of a positively charged ion [19].

Analyzing the Ni-O nanocluster from Table 3.1 complexes we conclude that a higher ionization potential indicates a higher energy requirement for electron removal, suggesting greater electron stability within the complexes [24].

Following graph represent the plotting of Ionisation potential of Ni-O Nanoclusters.
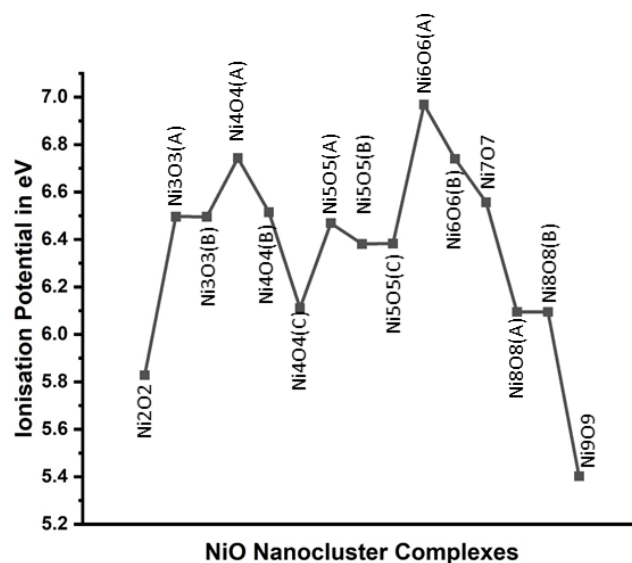

Fig 4.10. Graph showing variation of Ionisation Potential

Examining the calculated data of Ni-O nanocluster complexes from the Table 3.1 with different compositions for ionisation potential of Ni_nO_n (n=2-9),it can be observed that the ionization potentials range from 5.40 eV to 6.97 eV across the different nanocluster complexes. These values indicate the relative stability and electronic properties of each complex. Generally, structures with higher ionization potentials are less reactive and exhibit stronger electron stability [20].

4.4.2 ELECTRON AFFINITY

Electron affinity refers to the energy change that occurs when an atom or molecule gains an electron to form a negatively charged ion [25].

After analysing the data of electron affinity from Table 3.1 we can conclude that the electron affinity values for the Ni-O nanocluster complexes range from 3.69 eV to 5.75 eV, demonstrating variations in their ability to attract electrons.

Following is the graphical representation of electron affinity for Ni-O Nanoclusters.
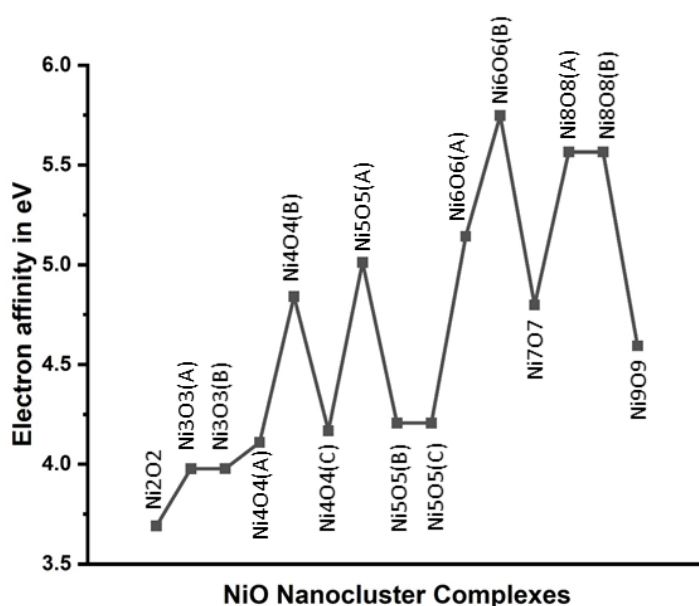

Fig 4.11. Graph showing variation of Electron affinity of Ni-O Nanoclusters

Among the complexes, Ni6O6(B) exhibits the highest electron affinity of **5.75 eV,** indicating its strong tendency to accept electrons compared to other complexes.

4.4.3 CHEMICAL POTENTIAL(μ)

$$\mu = -\frac{1}{2}(\epsilon_{LUMO} + \epsilon_{HOMO})$$

From Table 3.2 the chemical potential values (μ) for different Ni-O nanocluster complexes reflects the potential energy of the system's particles and provides insights into the system's stability and electron behaviour.

Analyzing the data, we can observe that the chemical potential values range from -4.7594 eV to -6.2438 eV for the different complexes. The negative values indicate the energy required to remove an electron from the system or the energy associated with adding an electron to the system.

A graph of the chemical potential values for the complexes would show a decreasing trend as the complexity of the nanocluster increases.
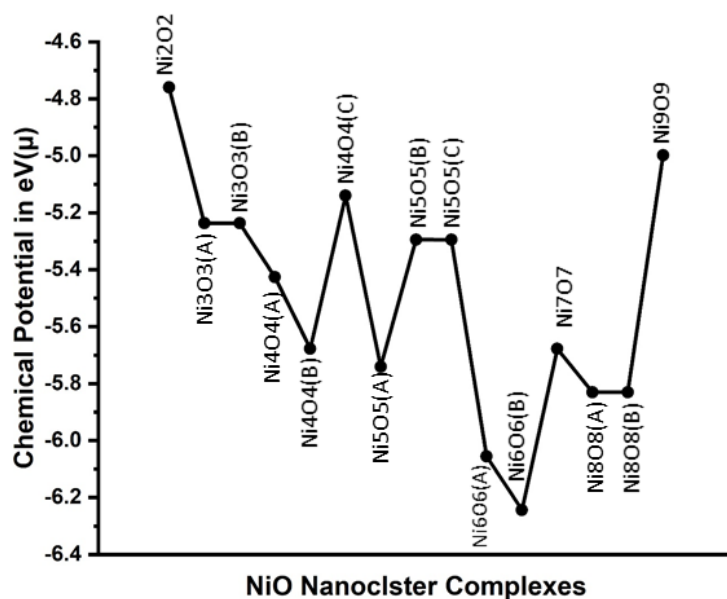

Fig 4.12. Graph showing variation of Chemical Potential for Ni-O Nanoclusters

Overall, the data indicates that the Ni-O nanocluster complexes exhibit varying degrees of stability and electron-attracting tendencies, as reflected by their respective chemical potential values.

4.4.4 GLOBAL HARDNESS(η)

$$\eta = \frac{1}{2}(\epsilon_{LUMO} - \epsilon_{HOMO})$$

Global hardness is a measure of the resistance of a system to changes in electron density. It provides insights into the stability and reactivity of the complexes.[26]

Analyzing the data from Table 3.2 for Global hardness, we can observe that the global hardness values range from 0.2645 eV to 1.31635 eV for the different complexes. The higher the hardness value, the greater the resistance to changes in electron density and the more stable the system.

A graph of the global hardness values for the complexes would show a variation in the hardness levels.
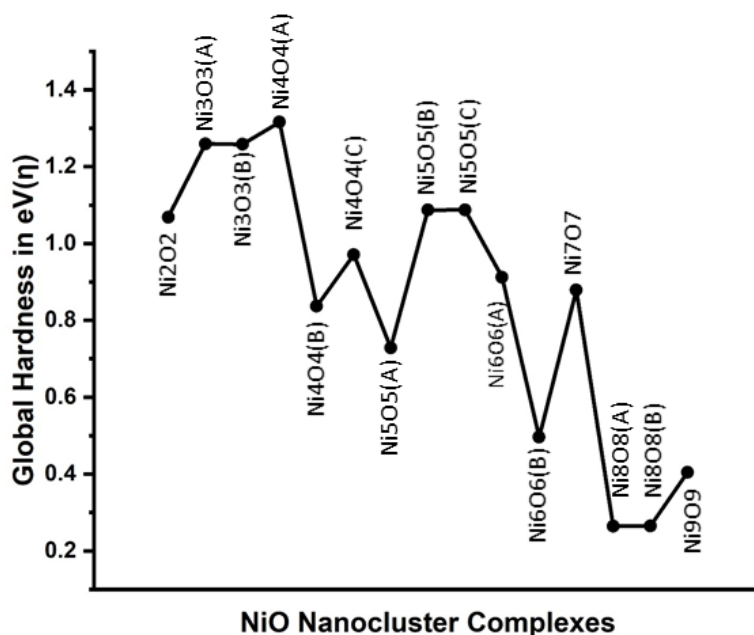

Fig 4.13. Graph showing variation of Global Hardness of Ni-O Nanoclusters

Some complexes have higher hardness values (e.g., Ni4O4(A) with a hardness of 1.31635 eV) indicating greater stability and resistance to electron density changes. On the other hand, complexes with lower hardness values (e.g., Ni8O8(A) with a hardness of 0.2645 eV) are relatively less stable and more susceptible to changes in electron density.

Overall, the data shows that the Ni-O nanocluster complexes exhibit varying degrees of stability and reactivity, as reflected by their global hardness values.

4.4.5 ELECTRONEGATIVITY (χ)

$$\chi = \frac{1}{2}(\epsilon_{LUMO} + \epsilon_{HOMO})$$

Electronegativity is a measure of the tendency of an atom to attract electrons towards itself in a chemical bond. It provides insights into the polarity and chemical behaviour of the complexes.[23].

Analyzing the data from Table 3.2, we can observe that the electronegativity values range from 4.7594 eV to 6.2438 eV for the different complexes. Higher electronegativity values indicate a stronger attraction for electrons and a higher tendency to pull electrons towards the atom.
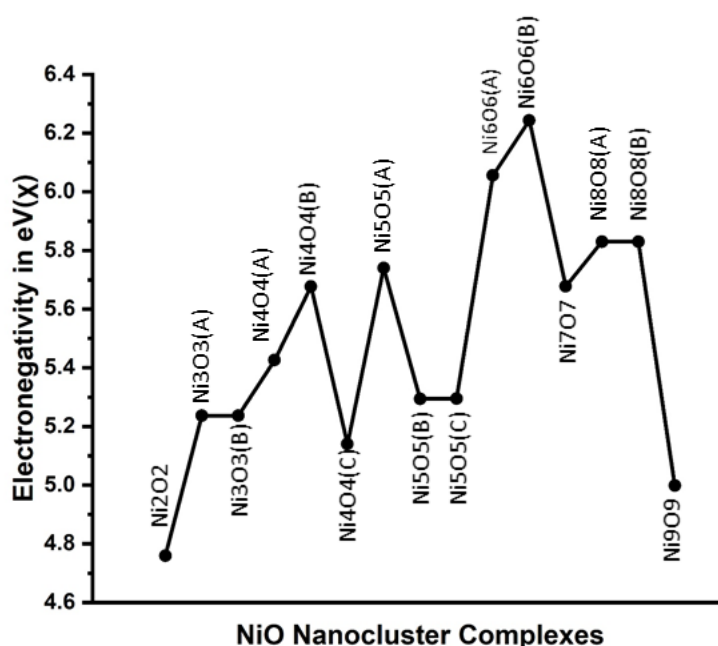

Fig 4.14 Graph showing variation of Electronegativity of Ni-O Nanoclusters

A graph of the electronegativity values for the complexes would show variation in electronegativity levels [27]. Some complexes have higher electronegativity values (e.g., Ni6O6(B) with an electronegativity of 6.2438 eV), indicating a stronger electron-attracting ability. On the other hand, complexes with lower electronegativity values (e.g., Ni2O2 with an electronegativity of 4.7594 eV) have a relatively weaker electron-attracting tendency.

Overall, the data shows that the Ni-O nanocluster complexes exhibit varying degrees of electronegativity, indicating different levels of electron-attracting tendencies and polarities.

4.4.6 GLOBAL SOFTNESS(S)

$$S = \frac{1}{2\eta}$$

Global softness is a concept in quantum chemistry that quantifies the reactivity and chemical softness of a system. It is inversely related to the hardness and reflects the ease with which a system can accept or donate electrons [24].

From Table 3.2, we can observe that the global softness values range from 0.3798 eV to 1.8904 eV for the different complexes. Higher global softness values indicate a greater reactivity and a higher tendency to accept or donate electrons [28].

Some complexes have higher softness values (e.g., Ni8O8(A) with a global softness of 1.8904 eV), indicating a higher reactivity and electron-donating ability.

On the other hand, complexes with lower softness values (e.g., Ni4O4(A) with a global softness of 0.3798 eV) have a relatively lower reactivity and electron-donating tendency.

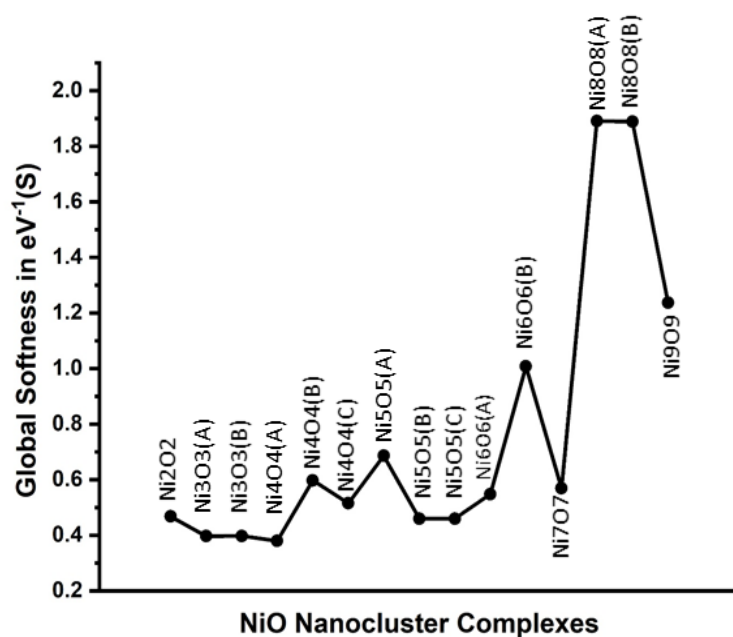A graph of the global softness values for the complexes would show variation in softness levels.

Fig 4.15. Graph showing variation of Global Softness of Ni-O Nanoclusters

Overall, the data shows that the Ni-O nanocluster complexes exhibit varying degrees of global softness, reflecting their reactivity and electron-donating or accepting abilities.

4.4.7 ELECTROPHILICITY INDEX (ω)

The electrophilicity index is a concept in computational chemistry that quantifies the electrophilic nature of a molecule or complex. It provides information about the ability of a system to accept electrons and engage in chemical reactions [25].

From Table 3.2, we can observe that the electrophilicity index values range from 10.5979 eV to 64.2512 eV for the different complexes. Higher electrophilicity index values indicate a stronger electrophilic character, implying a higher tendency to accept electrons and participate in reactions [26].

A graph of the electrophilicity index values for the complexes would show variation in electrophilic nature
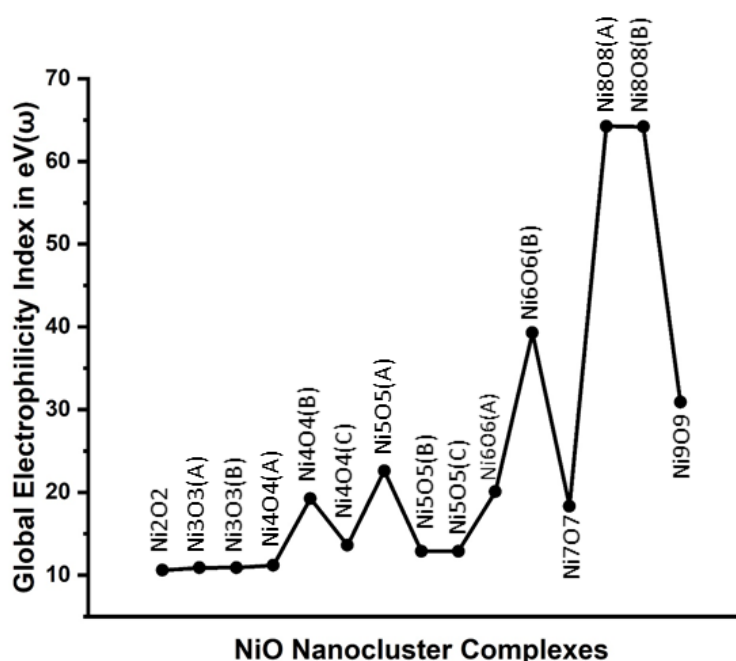

Fig 4.16 Graph showing variation of Electrophilicity Index of Ni-O Nanoclusters

Some complexes have higher electrophilicity index values (e.g., Ni9O9(A) with an electrophilicity index of 64.2512 eV), indicating a stronger electrophilic character and a

greater propensity to accept electrons. Conversely, complexes with lower electrophilicity index values (e.g., Ni2O2 with an electrophilicity index of 10.5979 eV) exhibit relatively lower electrophilicity and are less likely to accept electrons [29].

In summary, the data shows that the Ni-O nanocluster complexes exhibit varying degrees of electrophilicity, indicating their ability to accept electrons and engage in chemical reactions.

CHAPTER 5. CONCLUSION

Based on the provided data on the electronic properties of Ni-O nanocluster complexes, we can write the following conclusions:

The electronic properties of Ni-O nanocluster complexes offer valuable information about their stability, reactivity, and bonding behaviour. HOMO-LUMO gap values of the Ni-O nanoclusters range from 0.5290 to 2.6327 eV.

The values generally decrease as the size of the nanoclusters increases. One important parameter is the HOMO-LUMO gap in which complexes with higher HOMO-LUMO gaps tend to exhibit greater stability and lower reactivity, while those with lower gaps display higher reactivity.[30]

The chemical potential values of the Ni-O nanoclusters range from -6.2438 to -4.7594. The chemical potential becomes more negative as the size of the nanoclusters increases. This suggests that larger nanoclusters have a higher affinity for electrons, indicating a greater tendency to accept or gain electrons, it also indicate their electron-rich nature, making them prone to electron transfer or donation in chemical reactions. This property is advantageous for their involvement in redox processes and electron exchange [29].

The global hardness values of the Ni-O nanoclusters range from 0.2645 to 1.31635 ,and it provides insight into the stability and reactivity of the nanoclusters. The global hardness generally decreases as the size of the nanoclusters increases. Smaller nanoclusters, such as Ni4O4(C), Ni5O5(A), and Ni6O6(B), tend to have higher hardness values. Larger nanoclusters, such as Ni7O7 and Ni9O9(A), exhibit lower hardness values.The hardness values also show some variations within nanoclusters of the same size but different configurations. [31].

The relatively high electronegativity values across all complexes indicate their ability to attract electrons and form stable chemical bonds [30]. This characteristic highlights their potential for engaging in bonding interactions and participating in chemical reactions.

The data shows that the global softness values of the Ni-O nanoclusters range from 0.379838189 to 1.890359168. Softness is the reciprocal of hardness and provides information about the ease of deformation or electron excitation in a material. The

global softness generally increases as the size of the nanoclusters increases. Smaller nanoclusters, such as Ni4O4(A), Ni5O5(B), and Ni6O6(A), tend to have lower softness values, indicating higher resistance to deformation or electron excitation. Larger nanoclusters, such as Ni8O8(A) and Ni9O9(A), exhibit higher softness values, indicating easier deformation or electron excitation.

The wide range of electrophilicity index values among the complexes reflects variations in their electrophilic character [32]. Higher values signify a stronger tendency to accept electrons and participate in reactions as electrophiles.

In summary, these electronic properties provide crucial insights into the stability, reactivity, bonding behaviour, and potential applications of Ni-O nanocluster complexes. Understanding these properties is essential for tailoring and designing their behaviour for specific uses in catalysis, materials science, and other fields.

5.1 APPLICATIONS:

The Ni-O nanocluster complexes with larger HOMO-LUMO gaps and higher global hardness can be suitable for applications requiring stability and lower reactivity, such as catalysts in chemical reactions.

Complexes with higher electronegativity may find applications in electron transfer processes and as electrode materials in batteries or fuel cells [33].

Nanocluster complexes with higher global softness and electrophilicity index values can be employed in reactions involving electron donation or transfer, such as in organic synthesis or catalysis.

REFERENCES

[1]. Gary, Dylan C.; Flowers, Sarah E.; Kaminsky, Werner; Petrone, Alessio; Li, Xiaosong; Cossairt, Brandi M. (2016-02-10). "Single-Crystal and Electronic Structure of a 1.3 nm Indium Phosphide Nanocluster". Journal of the American Chemical Society. 138 (5): 1510–1513

[2]. T. Tsukuda and H. Häkkinen , Protected Metal Clusters: From Fundamentals to Applications , Elsevier, Amsterdam, 2015

[3]. Jiaojiao Han, Hao Li, Honglei Shen, Ying Xu, Xuejuan Zou, Xi Kang, Manzhou Zhu. (AuAg)44(SPhtBu)26 versus (AuAg)44(SPhF2)30: Tailoring the Geometric Structures and Optical Properties of Nanocluster Analogues.

[4] Qiao-Ling Mo, Bi-Jian Liu, Fang-Xing Xiao. Solar-Powered Photocatalysis and Photoelectrocatalysis over Atomically Precise Metal Nanoclusters. The Journal of Physical Chemistry

[5] C.C. Chen, A.B. Herhold, C.S. Johnson, A.P. Alivisatos, Science 276 (1997) 398.

[6] Y. Wang, J. Zhu, X. Yang, L. Lu, X. Wang, Thermochim. Acta 437 (2005) 106.

[7] Y.R. Uhma, J.H. Park, W.W. Kima, C.H. Chob, C.K. Rhee, Mater. Sci. Eng. B 106 (2004) 224.

[8] S.H. Lin, F.R. Chen, J.J. Kai, Appl. Surf. Sci. 254 (2008) 3357.

[9] X. Wang, J. Song, L. Gao, J. Jin, H. Zheng, Z. Zhang, Nanotechnology 16 (2005) 37.

[10] H. Sato, T. Minami, S. Takata, T. Yamada, Thin Solid Films 236 (1993) 27.

[11] V. Srinivasan, J. Weidner, J. Electrochem. Soc. 144 (1997) L210.

[12] J. He, H. Lindström, A. Hagfeldt, S.E. Lindquist, J. Phys. Chem. B 103 (1999) 8940.

[13] R. Cinnsealach, G. Boschloo, S.N. Rao, D. Fitzmaurice, Sol. Energy Mater. Sol. Cells 57 (1999) 107.

[14] K. Yoshimura, T. Miki, S. Tanemura, Jpn. J. Appl. Phys. 34 (1995) 2440. [11] C. Natarajan, H. Matsumoto, G. Nogami, J. Electrochem. Soc. 144 (1997) 121.

[15] C.S. Carney, C.J. Gump, A.W. Weimer, Mater. Sci. Eng. A 431 (2006) 1.

[16] A. Surca, B. Orel, B. Pihlar, P. Bukovec, J. Electroanal. Chem. 408 (1996) 83.

[17] J.H. Liang; Y.D. Li, Chem. Lett. 32 (2003) 1126.

[18] Z.H. Liang, Y.J. Zhu, X.L. Hu, J. Phys. Chem. B 108 (2004) 3488.

[19] D.N. Yang, R.M. Wang, J. Zhang, Z.F. Liu, J. Phys. Chem. B 108 (2004) 7531.

[20] R.H. Kodama, S.A. Makhlouf, A.E. Berkowitz, Phys. Rev. Lett. 79 (1997) 1393.

[21] M.H. Shah, Nanoscale Res. Lett. 3 (2008) 255.

[22] P. Palanisamy, A.M. Raichur, Mater. Sci. Eng. C 29 (2009) 199.

[23] X. Song, L. Gao, J. Am. Ceram. Soc. 91 (2008) 3465.

[24] S. Rodríguez-Llamazares, J. Merchán, I. Olmedo, H.P. Marambio, J.P.Muñoz, P. Jara, J.C. Sturm, B. Chornik, O. Peña, N. Yutronic, M.J. Kogan, J. Nanosci. Nanotech. 8 (2008) 3820.

[25] B. Corain, G. Schmid, N. Toshima (Eds.), Catalysis and Materials Science: The Issue of Size Control, Elsevier Publishers, Oxford, 2008, p. 21.

[26] J. Park, E. Kang, S.U. Son, H.M. Park, M.K. Lee, J. Kim,

[27] M. Salavati-Niasari, F. Davar, M. Mazaheri, M. Shaterian, J. Magn. Magn. Mater. 320 (2008) 575.

[28] H.T. Yang, Y.K. Su, C.M. Shen, T.Z. Yang, H.J. Gao, Surf. Interf. Anal. 36 (2004)155.

[29] K. Nakamoto, Infrared and Raman spectra of Inorganic and Coordination Compounds, 4th Ed., Wiley, VCH, 1986, p. 245.

[30] M. Salavati-Niasari, Z. Fereshteh, F. Davar, Polyhedron 28 (2009) 126.

[31] M. Salavati-Niasari, F. Davar, N. Mir, Polyhedron 27 (2008) 3514.

[32] G. Boschloo, A. Hagfeldt, J. Phys. Chem. B 105 (2001) 3039.

[33] T. Tsuboi, W. Kleeman, J. Phys.: Condens. Matter 6 (1994) 8625